CHAPTER-10

ELECTRON ACCELERATION BY HERMITE GAUSSIAN LASER BEAM IN PLASMA: ROLE OF TEM MODES

10.1 INTRODUCTION

The intensity distribution of laser beam in its propagation region is important because it determines the laser-plasma interaction process. Intensity varying two regimes exist [8]. First, the lower intensity where laser field is weak and net kinetic energy gain by electron remains lower. Second, the higher intensity where laser field is stronger and electron energy gain as well as acceleration is higher. Accordingly the electron trapped in laser field gets accelerated to high energy due to laser. The laser beam parametric variations have been investigated theoretically and several experimental models have been presented for high energy gain by electrons [5, 21, 45, 60, 79, 111]. In an experiment with laser-driven plasma accelerator, the acceleration gradient of about $10GeV/m$ was reported with emergence of a mono-energetic and low divergence electron beams in $100MeV-1GeV$ range [5]. Fortin et al. [91] studied the dependence of energy gained by electron on the power of laser, laser beam waist, and duration of pulse for electron acceleration. Gaussian profile of laser pulse proves its suitability for electron acceleration because of its ability to generate high energy, narrow divergence electron beams of constricts energy spread [91]. The fields of lowest order RP Gaussian laser beam were employed to accelerate electrons to energy range of GeV [61, 66]. The Gaussian beam fields are determined by laser beam frequency ω, radius of beam waist r_0 at the focus, and Rayleigh length $Z_R = kr_0^2/2$. Feng *et al.* [49] studied the vacuum acceleration of electron with a Gaussian laser pulse. They proposed that the evolution of the laser beam waist cannot be ignored when the electron drifting distance is of the order of Rayleigh length. Thus, the electron can efficiently be accelerated and drawn out by the longitudinal ponderomotive force due to Gaussian laser beam. The electron energy gain of few MeV was realized with a Gaussian laser beam of intensity above $10^{19}W/cm^2$.

Propagation properties of Gaussian laser beams directly influence the electron acceleration. The mode index influenced intensity variations were investigated and reported [24, 114, 124]. Recently, Flaco *et al.*[125] conducted an experiement using Hermite-Gaussian (HG) laser beam with distinct modes. They reported a persisting magnetic field driven by relativistics elecctrons in plasma.

In this chapter we present the influence of different mode indices of Hermite polynomial on electron acceleration by using a relativistic 3-D single particle code with CP HG laser beam in plasma. We investigate the effect of laser beam width parameter and mode indices of HG laser beam on electron acceleration with variation of laser intensity. High energy gain is realized in the presence of high intensity laser pulse. We compare the acceleration distance in term of Rayleigh length for different values of laser beam spot size. The greater count of Rayleigh length in terms of propagation distance is observed for a smaller beam spot size and vice versa. The electron gain high energy with small beam width parameter due to strong laser field and loss energy with large beam width due to weak field with large propagation distance. The content of rest part of this paper is arranged as follows. Section 10.2 explains the electromagnetic fields of a HG laser beam, section 10.3 explains the distinct modes with intensity of HG laser beam, and section 10.4 presents the electron dynamics required to study electron acceleration. Outcomes are discussed in section 10.5. Finally, conclusion is drawn in the section 10.6.

10.2 FIELD DISTRIBUTION FOR A HERMITE GAUSSIAN BEAM

The transverse electric field components for a CP Hermite Gaussian laser beam propagating in the z-direction, under paraxial approximation can be written as [49, 61, 66, 91]:

$$E_x(r,z,t)=\frac{E_0}{f(z)}\exp(i\phi)H_m\left(\frac{\sqrt{2}}{r_0 f(z)}x\right)\exp\left(-\frac{(t-\frac{z-z_L}{c})^2}{\tau^2}-\frac{r^2}{r_0^2 f^2}\right), \qquad (10.1)$$

$$E_y(r,z,t)=\frac{E_0}{f(z)}\exp\left[i\left(\phi+\frac{\pi}{2}\right)\right]H_n\left(\frac{\sqrt{2}}{r_0 f(z)}y\right)\exp\left(-\frac{(t-\frac{z-z_L}{c})^2}{\tau^2}-\frac{r^2}{r_0^2 f^2}\right), \quad (10.2)$$

where E_0 is the amplitude of electric field of HG laser beam; ϕ is the HG beam phase; $H_{m,n}$ is the Hermite-polynomial function; m,n are the mode indices associate with Hermite-polynomial; τ is the pulse duration; z_L is the initial position of the pulse peak, $r^2=x^2+y^2$; r_0 is the minimum laser spot size, and c is the velocity of light in vacuum. $f(z)$ is the laser beam width parameter and can be expressed as:

$$f(z)=\sqrt{1+\xi^2}\,, \quad (10.3)$$

where $\xi=z/Z_R$ is the normalized propagation distance, $Z_R=kr_0^2/2$ is the Rayleigh length, k is the laser wave number, $\phi=\omega_0 t-kz+(\mathrm{m}+\mathrm{n}+1)\tan^{-1}(\xi)-zr^2/(Z_R r_0^2 f^2)+\phi_0$, ω_0 is the laser frequency, $(\mathrm{m}+\mathrm{n}+1)\tan^{-1}(\xi)$ is the Guoy phase, and ϕ_0 is the initial phase.

To express the laser fields correctly, in addition to transverse electric components, the longitudinal electric component and magnetic components are express by paraxial ray approximation as:

$$E_z(r,z,t)=-\left(\frac{i}{k}\right)\left(\frac{\partial E_x}{\partial x}+\frac{\partial E_y}{\partial y}\right), \quad (10.4)$$

$$\vec{B}(r,z,t)=-\left(\frac{i}{\omega}\right)\left(\vec{\nabla}\times\vec{E}\right). \quad (10.5)$$

We have considered a plasma with a density about $10^{23}m^{-3}$, and a laser pulse of the wavelength $\lambda=1.054\mu m$. Therefore, the plasma frequency and the frequency of laser pulse are $\omega_p=1.8\times10^{13}rad/s$ and $\omega_0=1.8\times10^{15}rad/s$ respectively. Hence, $\omega_p^2/\omega_0^2\approx10^{-4}$. It has been experimentally proved that at this plasma density (with pressure $\approx1Torr$), plasma effects such as wake-fields, plasma instabilities, and modification of amplitude can be neglected [32].

10.3 INTENSITY DISTRIBUTION FOR DIFFERENT MODES OF HG BEAM

For a Hermite polynomial $H_{m,n}(\sqrt{2}r/r_0 f(z))$, the intensity of CP HG laser beam is expressed as:

$$I(r,z,t) = I_0\left[\frac{E_0}{f(z)} H_m\left(\frac{\sqrt{2}}{r_0 f(z)}x\right) H_n\left(\frac{\sqrt{2}}{r_0 f(z)}y\right)\exp\left(-\frac{(t-\frac{z-z_L}{c})^2}{\tau^2}-\frac{r^2}{r_0^2 f^2}\right)\right]^2 . \quad (10.6)$$

The intensity of CP HG laser beam for different mode indices has been obtained by using eq. (10.6). We write the Hermite polynomial and intensity proportionality with different mode indices for a CP HG laser beam in Table 10.1

Table 10.1. Hermite polynomials (H_m, H_n) and Intensity factor $I \propto (H_m H_n)^2$ with different mode indices (m, n) for CP HG laser beam

Mode Indices	Hermite polynominals		Proportionality factor of Intensity
(m,n)	$H_m\left(\frac{\sqrt{2}}{r_0 f(z)}x\right)$	$H_n\left(\frac{\sqrt{2}}{r_0 f(z)}y\right)$	$I \propto (H_m H_n)^2$
(0,0)	1	1	1
(0,1)	1	$\frac{2\sqrt{2}y}{f(z)r_0}$	$\frac{8y^2}{f^2(z)r_0^2}$
(0,2)	1	$\frac{8y^2}{f^2(z)r_0^2}-2$	$\frac{64y^4}{f^4(z)r_0^4}-\frac{32y^2}{f^2(z)r_0^2}+4$
(0,3)	1	$\frac{\sqrt{2}y}{f(z)r_0}\left(\frac{16y^2}{f^2(z)r_0^2}-12\right)$	$\frac{4y^2}{f^2(z)r_0^2}\left(\frac{16y^4}{f^4(z)r_0^4}-\frac{24y^2}{f^2(z)r_0^2}+9\right)$
(0,4)	1	$\frac{64y^4}{f^4(z)r_0^4}-\frac{96y^2}{f^2(z)r_0^2}+12$	$\left(\frac{64y^4}{f^4(z)r_0^4}-\frac{96y^2}{f^2(z)r_0^2}+12\right)^2$

HG modes are designated as transverse electromagnetic modes i.e. TEM_{mn}. The lowest order HG mode is TEM_{00}. This mode represents a Gaussian beam. The Guoy phase of a TEM_{mn} mode is stronger than that of the TEM_{00} mode by a factor $m+n+1$.

10.4 ELECTRON DYNAMICS AND RELATIVISTIC ANALYSIS

The momentum and energy of electron are expressed in terms of following equations:

$$\frac{dp_x}{dt} = -eE_x + e\beta_z B_y - e\beta_y (B_z), \tag{10.6}$$

$$\frac{dp_y}{dt} = -eE_y - e\beta_z B_x + e\beta_x (B_z), \tag{10.7}$$

$$\frac{dp_z}{dt} = -eE_z - e(\beta_x B_y - \beta_y B_x), \tag{10.8}$$

$$\frac{d\gamma}{dt} = -e(\beta_x E_x + \beta_y E_y + \beta_z E_z), \tag{10.9}$$

where (p_x, p_y, p_z) are the (x, y, z) coordinates of the momentum $\vec{p} = \gamma m_0 \vec{v}$; $(\beta_x, \beta_y, \beta_z)$ are the (x, y, z) coordinates of the normalized velocity $\vec{\beta} = \vec{v}/c$; $\gamma^2 = 1 + (p_x^2 + p_y^2 + p_z^2)/(m_0 c)^2$ is the Lorentz factor, $-e$ and m_0 are the charge and rest mass of electron respectively.

The dimensionless variables are expressed as follow:

$$a_0 \to \frac{eE_0}{m_0 \omega_0 c},\ \tau' \to \omega_0 \tau,\ r_0' \to \frac{\omega_0 r_0}{c},\ z_L' \to \frac{\omega_0 z_L}{c},\ x' \to \frac{\omega_0 x}{c},\ y' \to \frac{\omega_0 y}{c},\ z' \to \frac{\omega_0 z}{c},$$

$$\beta_x \to \frac{v_x}{c},\ \beta_y \to \frac{v_y}{c},\ \beta_z \to \frac{v_z}{c},\ t' \to \omega_0 t,\ p_0' \to \frac{p_0}{m_0 c},\ p_x' \to \frac{p_x}{m_0 c},\ p_y' \to \frac{p_y}{m_0 c},$$

$p_z' \to \frac{p_z}{m_0 c}$, and $k' \to \frac{ck}{\omega_0}$.

Equations (10.6)-(10.9) are the coupled differential equations. These equations have been solved numerically with a computer simulation code for electron energy.

10.5 RESULTS AND DISCUSSION

We have chosen the following dimensionless parameters for numerical analysis: $a_0 = 5$ (represents laser intensity $I \sim 6.92 \times 10^{19}\ W/cm^2$), $a_0 = 25$ (represents laser intensity $I \sim 8.5 \times 10^{20}\ W/cm^2$), $a_0 = 50$ (represents laser intensity $I \sim 6.8 \times 10^{21}\ W/cm^2$); $r_0' = 150$ (represents laser spot size $r_0 \sim 25\mu m$), $r_0' = 300$ (represents laser spot size $r_0 \sim 50\mu m$), $r_0' = 450$ (represents laser spot size $r_0 \sim 75\mu m$), $\tau_L' = 70$(corresponding to laser pulse duration of $200fs$); initial position of pulse peak $z_L' = 0$; initial electron position $x_i' = 0$, $y_i' = 0$, and $z_i' = 0$; initial phase $\phi_0 = 0$, normalized initial momentum of electron $p_0' = 1$.

Figure 10.1 represents the variation of electron energy gain with respect to normalized propagation distance ξ for the mode $(m,n) = (0,1)$. This gain has been examined for distinct values of laser spot size r_0' with intensity parameters $a_0 = 5$, 25, and 50. Higher energy gain appears with higher intensity for same spot size. Fig. 10.1(b) depicts energy gain of about $600MeV$ with $a_0 = 50$ and $r_0' = 150$. Hartemann *et al.* [8] reported that role of the beam focus for achieving the high energy accelerating particle. In chapter 9, the role of beam width parameter has been explained for achieving the accelerating distance of the order of Rayleigh length with a focused Gaussian beams. From figures 10.1(c), one can observe the acceleration distance of about six times the Rayleigh length with $r_0' = 300$. We have plotted the variation of laser beam width parameter $f(z)$ with respect to normalized propagation distance and observe an increase in the beam width parameter with the distance of propagation of laser pulse in plasma. Smaller the beam width parameter stronger the electron acceleration and vice versa. Hence, high acceleration is observed with a small beam width parameter.

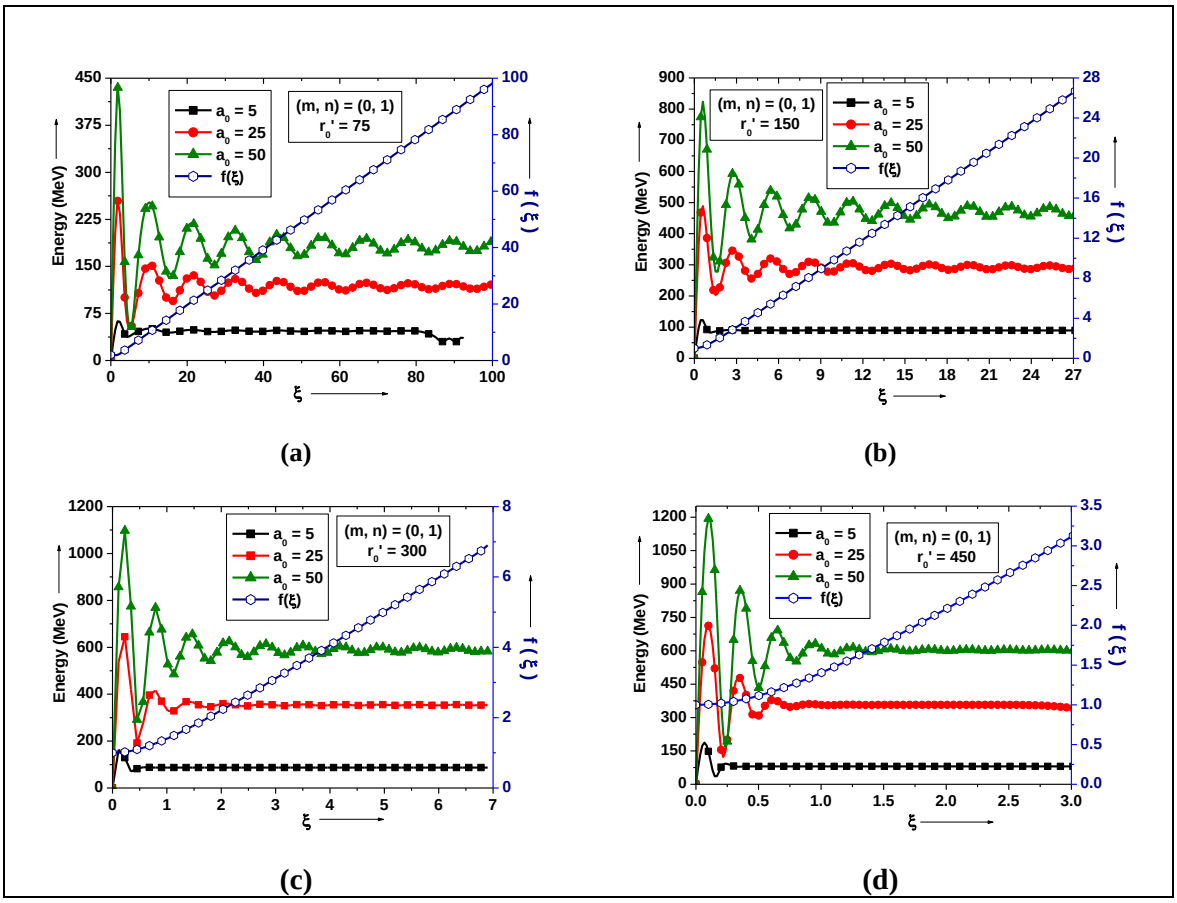

Figure. 10.1. Variation plot for electron energy gain for the mode $(m,n)=(0,1)$ **with normalized propagation distance** ξ **and beam width parameter** $f(z)$ **for the distinct values of laser spot size** r_0' **and intensity parameters** $a_0=5$, 25, **and** 50. **(a)** $r_0'=75$, **(b)** $r_0'=150$, **(c)** $r_0'=300$, **and (d)** $r_0'=450$. **The other parameters are** $\tau_L'=70$, $\phi_0=0$, $p_0'=1$, $z_L'=0$, $x_i'=0$, $y_i'=0$, **and** $z_i'=0$.

We observe the acceleration and deceleration of electron while interaction with a HG laser pulse in plasma. It is due to the asymmetry in intensity of CP HG laser beam. This enforces the trapping and acceleration of electron for longer distance. The electron first gain high energy during interaction with the leading part of pulse. The gain saturates till reaching to the trailing part of pulse.

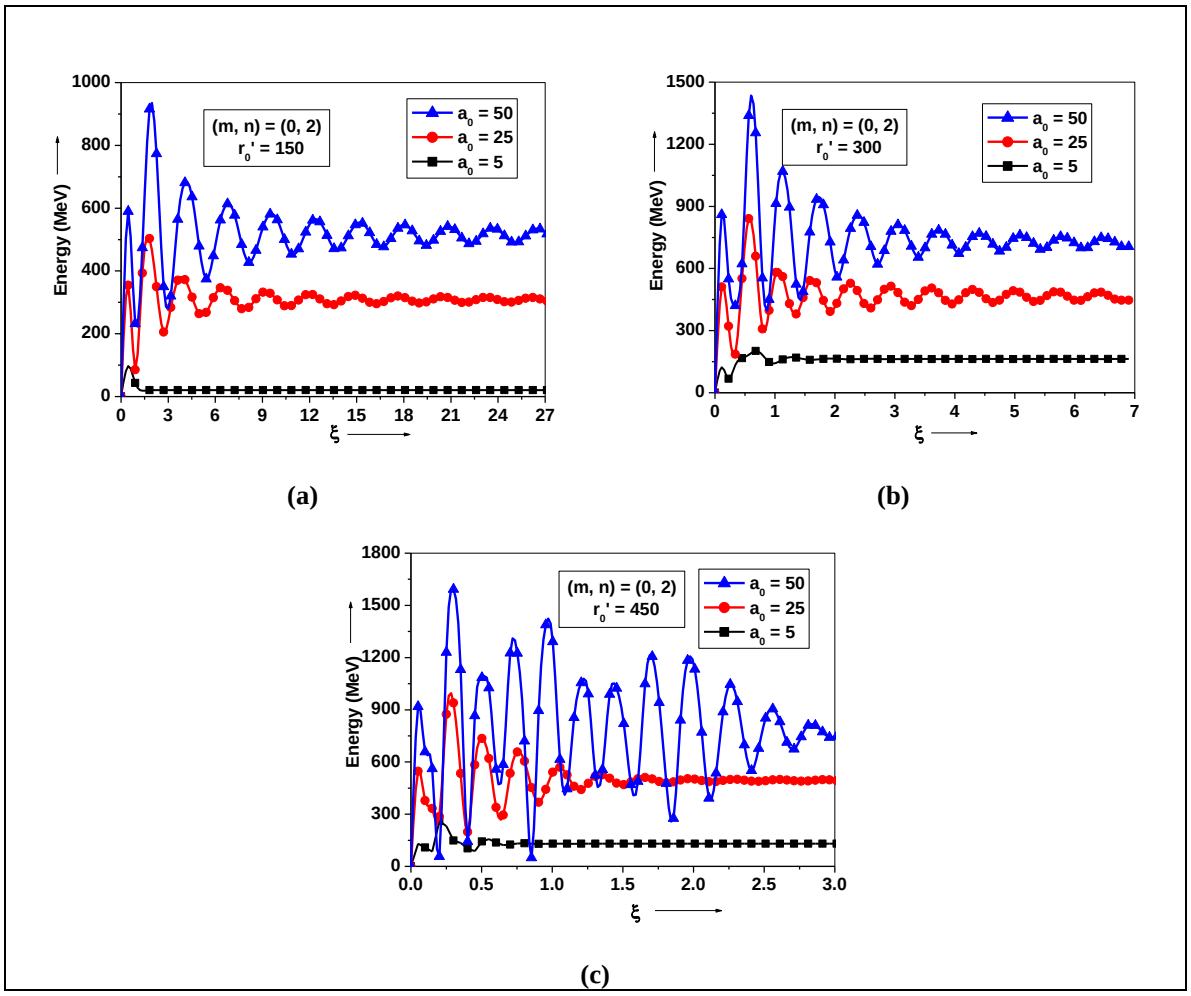

Figure 10.2. Variation plots for electron energy gain for the mode $(m,n)=(0,2)$ with normalized propagation distance ξ for distinct values of intensity parameter $a_0=5$, 25 and 50 with laser spot size: (a) $r_0'=150$, (b) $r_0'=300$, and (c) $r_0'=450$. Rest of the parameters are as referred in fig. 10.1.

In chapter 4, the electron accelerating distance calculated is about three times the Rayleigh length with a LP chirped laser pulse of a large spot size $r_0'=900$ in vacuum. One can observe the acceleration distance with a CP HG laser pulse is about six times the Rayleigh length for a smaller initial laser spot size $r_0'=300$ in plasma.

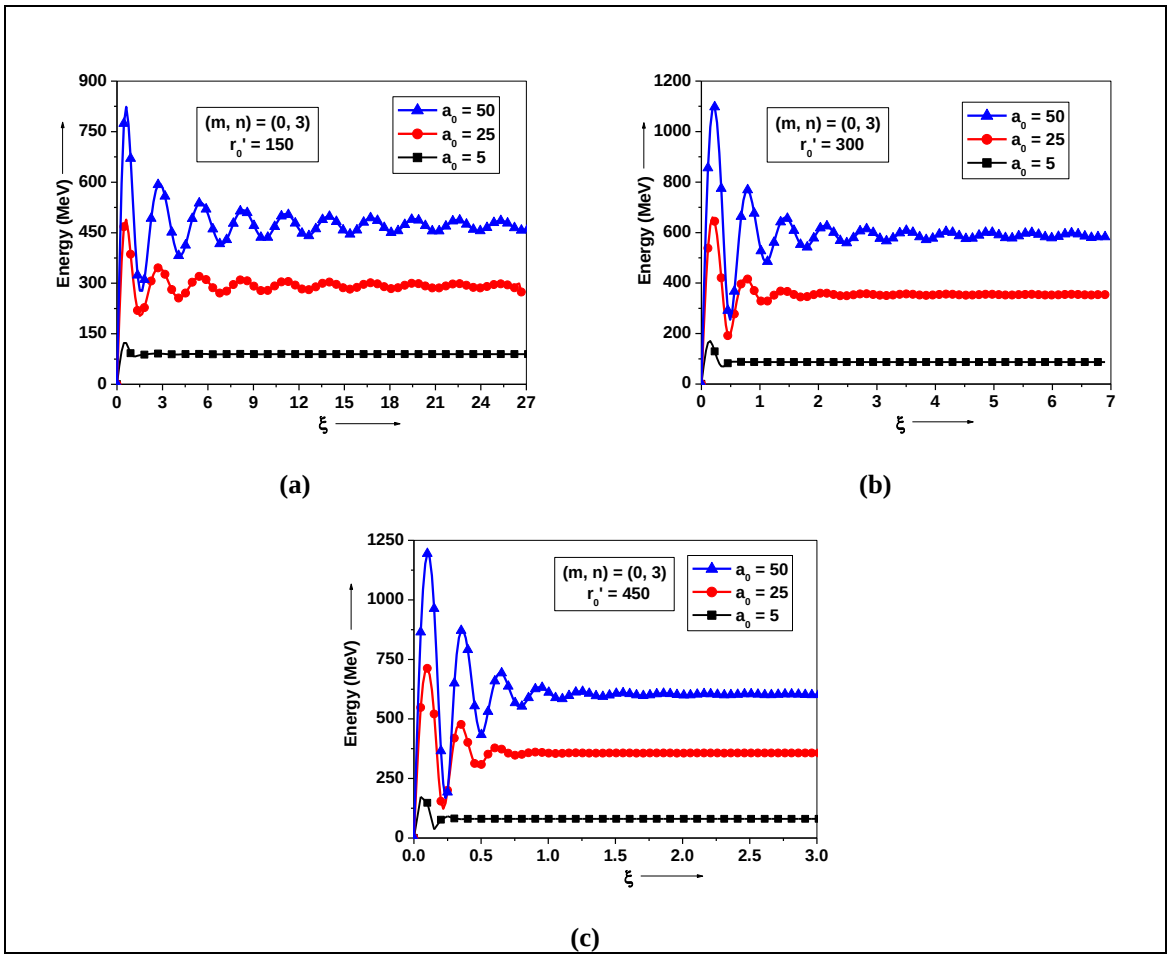

Figure 10.3. Variation plots for electron energy gain for the mode $(m,n)=(0,3)$ with normalized propagation distance ξ for distinct values of intensity parameter $a_0=5$, 25 and 50 with laser spot size: (a) $r_0'=150$, (b) $r_0'=300$, and (c) $r_0'=450$. Rest of the parameters are as referred in fig. 10.1.

It is the betatron resonance which set up between accelerating electron and laser pulse during laser electron interaction in plasma. Figure 10.1(d) presents the electron energy gain with a large beam spot size. In such case the wider acceleration and deceleration appears. The electron is accelerated where laser field strength is high in the vicinity of sharp focus and decelerates where laser field strength is weak. This makes an effective acceleration of electron in plasma.

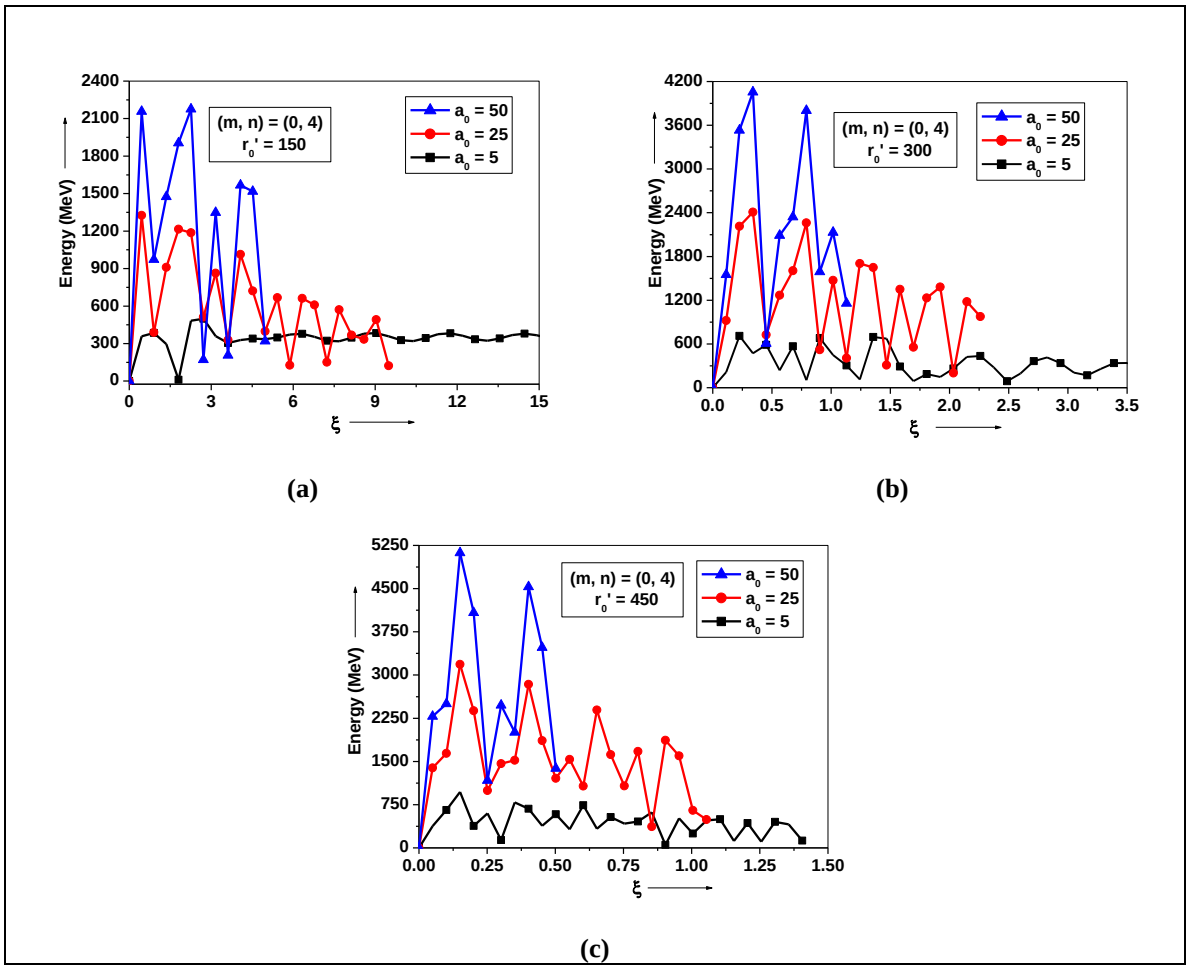

Figure 10.4. Variation plots for electron energy gain for the mode $(m,n)=(0,4)$ with normalized propagation distance ξ for distinct values of intensity parameter $a_0=5$, 25 and 50 with laser spot size: (a) $r_0'=150$, (b) $r_0'=300$, and (c) $r_0'=450$. Rest of the parameters are as referred in fig. 10.1.

Figure 10.2 represents the variation plots for electron energy gain as a function of ξ for distinct intensity parameters and normalized laser spot size for the mode index $(m,n)=(0,2)$. The variation has been plotted graphically for different intensity parameters $a_0=5$, 25, and 50. After reaching to the maximum energy gain, the electron decelerates slightly due to weakening of field with increasing beam width parameter. The electron energy gain then saturates. The electron retains significant amount of energy even in the

weak laser field. One can observe from Fig. 10.2(a), (b), and (c), that the accelerated electron retains high energy for larger distance.

Figure 10.3 and 10.4 represent the variation plots for electron energy gain with respect to the normalized propagation distance ξ for distinct intensity parameters and normalized laser spot size for the mode indices $(m,n)=(0,3)$ and $(m,n)=(0,4)$. In Fig. 10.3(b) and 10.3(c), we see the variation for two different values of laser spot size $r_0'=300$ and 450. The electron energy gain first increases while interaction with laser pulse. After attaining the maximum energy value, the electron is decelerated due to increasing laser beam width parameter and then energy gain is saturated for larger distances. An energy gain of the order of $1GeV$ is achieved with laser intensity $a_0=50$ (corresponding to $I\sim 6.8\times10^{21}\ W/cm^2$) and spot size $r_0'=300$. The electron energy gain greater than $1GeV$ is achieved with same intensity, and larger spot size $r_0'=450$. We have calculated the accelerating distance of electron which is about three times the Rayleigh length. We find that with higher modes the electron gains higher energy quickly. However, retains a smaller portion of energy for larger distance. This is due to the variation of intensity with higher modes, which results a weak field at longer distance. Hence, the electron loss energy even with high modes at larger distance.

10.6 CONCLUSION

In this study we have highlighted the importance of laser beam width parameter of a CP HG laser beam on electron energy gain in plasma. We have noticed an enhanced electron energy gain above $1GeV$ for laser intensity $a_0=50$ (corresponding to $I\sim 6.8\times10^{21}\ W/cm^2$) with laser spot size $r_0'=450$ ($\sim 75\mu m$) with modes upto $(0,2)$. We have also observed the role of different modes on the electron energy gain. Though, the energy gain with higher modes remains high but the electron de-phased at shorter distance. With an appropriate selection of laser beam spot size, and mode index, the electron can be accelerated to the order of GeV energy.